postulated that the solution dimer and the solid complexes isolated from approximately neutral solutions share a di-μ-cystinato-dicopper(II) structural feature. The present structure supports their suggestion, although polymeric[19] Cu(II) cystinate complexes cannot definitely be excluded. Both cis and trans copper(II) L-cystinate complexes have been isolated and characterized in our laboratories. These studies will be published elsewhere.[20]

Acknowledgment. This work was supported by the Research Corporation (H. J. S.), the Rutgers Biomedical Sciences Support Grant sponsored by the National Institutes of Health (H. J. S.), the Rutgers Research Council (H. J. S.), and the Rutgers Computing Center (H. J. S., J. P.). Predoctoral fellowships from Lever Brothers (J. A. T.) and National Science Foundation (D. M.) are gratefully acknowledged. We thank Dr. G. D. Benson of the Jefferson Medical School for stimulating discussions and Merck and Co., Inc., for a gift of D-penicillamine.

(19) D. Otto, G. Ferenc, and M. Tamas, *Magy. Kem. Foly.*, 68, 1 (1962); *Chem. Abstr.*, 57, 172*f* (1962).

(20) J. A. Thich, D. Mastropaolo, J. Potenza, and H. J. Schugar, to be submitted for publication.

Supplementary Material Available. A listing of structure factor amplitudes will appear following these pages in the microfilm edition of this volume of the journal. Photocopies of the supplementary material from this paper only or microfiche (105 × 148 mm, 24× reduction, negatives) containing all of the supplementary material for the papers in this issue may be obtained from the Journals Department, American Chemical Society, 1155 16th St., N.W., Washington, D. C. 20036. Remit check or money order for $3.00 for photocopy or $2.00 for microfiche, referring to code number JACS-74-726.

Porphyrin–Annulene Redox-Related Ligand Pair. Electrochemical Synthesis and Characterization of the Reduction Products of the Cobalt, Copper, and Nickel Complexes of a Tetraaza[16]annulene

Nurhan Takvoryan, Keith Farmery, Vladimir Katovic, Frank V. Lovecchio, Ernest S. Gore, Larry B. Anderson, and Daryle H. Busch*

Contribution from the Evans Chemical Laboratories, The Ohio State University, Columbus, Ohio 43210. *Received September 6, 1973*

Abstract: $Co^{II}(TAAB)^{2+}$, $Ni^{II}(TAAB)^{2+}$, and $Cu^{II}(TAAB)^{2+}$ undergo successive one-electron electrochemical reductions to form stable complexes which have been formulated as derivatives of the dianionic ligand $TAAB^{2-}$, a porphyrin analog. The reactants contain the well-characterized annulene-like ligand tetrabenzo[*b*,*f*,*j*,*n*][1,5,9,13]-tetraazacyclohexadecine. The reduction products, which are tentatively assigned the formulations $[Co^{III}(TAAB^{2-})]ClO_4$, $[Co^{II}(TAAB^{2-})]CH_3CN$, $[Ni^{III}(TAAB^{2-})]ClO_4$, $[Ni^{II}(TAAB^{2-})]^0$, and $[Cu^{III}(TAAB^{2-})]ClO_4$, have been synthesized by controlled potential electrolysis and, in some cases, by chemical means and characterized by the usual chemical and physical measurements. Voltammetric studies at dme and rpe and cyclic voltammetric studies have been carried out on all these compounds in methanol and acetonitrile. The reduced complexes of cobalt have a unique electrochemistry which considerably strengthens the suggestion that they possess electronic and structural characteristics which differ significantly from that of the parent $Co^{II}(TAAB)^{2+}$ complex and that they should be formulated as complexes of the dianion ligand, $TAAB^{2-}$. The dramatic rearrangement to $Co^{III}(TAAB^{2-})^+$ is thought to proceed relatively slowly *via* a $Co^{I}(TAAB)^+$ intermediate. The lifetime of this intermediate is sufficiently long to facilitate its detection and characterization by electrochemical and spectral measurements. The $Co^{III}(TAAB^{2-})^+$ complex can be reoxidized to the original $Co^{II}(TAAB)^{2+}$ using cyclic voltammetry. The relationship between the annulene TAAB and the two-electron oxidation product of the porphyrin dianion is clarified.

Metalloporphyrins exhibit a rich oxidation–reduction chemistry and a number of studies[1-5] have revealed their general tendency to undergo multiple one-electron oxidation processes. A point of particular interest to us at this time is the conclusion that the ligand in various metalloporphyrins undergoes a total of two one-electron oxidations. We assert that the 16-membered great ring of the two-electron oxidation product is essentially an analog of [16]annulene, *i.e.*, a tetraaza[16]annulene (I). It follows that the chemistry of the product chelates should be that of tetraazaannulene complexes.

Similarly, the two-electron reduction product of the related pure organic chemical system, [16]annulene,[6] should provide an analog for the parent porphyrin. Oth and coworkers[7] found that [16]annulene itself

(1) A. Wolberg and J. Manassen, *J. Amer. Chem. Soc.*, 92, 2982 (1970).

(2) A. Stanienda and G. Biehl, *Z. Phys. Chem. (Frankfurt am Main)*, 52, 254 (1967).

(3) J. Fajer, D. C. Borg, A. Forman, D. Dolphin, and R. H. Felton, *J. Amer. Chem. Soc.*, 92, 3451 (1970).

(4) D. Dolphin, R. H. Felton, D. C. Borg, and J. Fajer, *J. Amer. Chem. Soc.*, 92, 743 (1970).

(5) R. H. Felton, D. Dolphin, D. C. Borg, and J. Fajer, *J. Amer. Chem. Soc.*, 91, 196 (1969).

(6) F. Sondheimer and Y. Gaoni, *J. Amer. Chem. Soc.*, 83, 4863 (1961).

(7) J. F. M. Oth, G. Anthoine, and J. M. Gilles, *Tetrahedron Lett.*, 60, 6265 (1968); J. F. Oth, H. Baumann, J. M. Gilles, and G. Schroder, *J. Amer. Chem. Soc.*, 94, 3498 (1972).

Table I. Electrochemical Reductions of M(TAAB)$^{2+}$ Complexes in MeOH[a]

Complex	Electrolyte	$E_{1/2}(1)$	$E_{1/2}(2)$	$E_{1/2}(3)$	$E_{1/2}(4)$	$E_{1/2}(5)$	$E_{1/2}(6)$	Σ[b]
$Co(TAAB)Br_2 \cdot H_2O$	TEAP	−0.54 (1)	−0.88 (1)	−0.07 (1)	−1.24	−1.42	−1.61	~9
$Co(TAAB)(Cl)_2$	TEAP	−0.55 (1)	−0.90 (1)	−1.05 (1)	−1.22	−1.43		~8
$Co(TAAB)I_2$	TEAP	−0.54 (1)	−0.88 (1)	−1.07 (1)	−1.23	−1.42	−1.63	~10
$Co(TAAB)(NCS)_2$	TEAP	−0.54 (1)	−0.88 (1)	−1.06 (1)	−1.23	−1.43		~8
$Co(TAAB)(BF_4)_2$	TEAP	−0.55 (1)	−0.87 (1)	−1.07 (1)	−1.23	−1.43	−1.63	~8
$Co(TAAB)(BPh_4)_2$	TEAP	−0.55 (1)	−0.89 (1)	−1.07 (1)	−1.24	−1.43	−1.63	~10
$Co(TAAB)(ClO_4)_2 \cdot H_2O$	KNO_3	−0.54 (1)	−0.89 (1)	−1.15 (1)	−1.32	−1.54	−1.70	~8
$Co(TAAB)(NO_3)_3$	TEAP	−0.55 (1)	−0.89 (1)	−1.07 (1)	−1.23	−1.44	−1.65	~8
$Ni(TAAB)(Cl)_2$	KCl	−0.43 (1)	−0.62 (1)		−1.57 (8)			10
$[Ni(TAAB)(OCH_3)_2]$	KCl	−0.50 (1)			−1.54 (5)			6
$Ni(H_8TAAB)(Cl)_2$	KCl	−0.97 (2)						2
$Cu(TAAB)(NO_3)_2$	KNO_3	+0.06 (1)			−1.00 (c)			
$CuTAAB(OCH_3)_2$	KNO_3	−0.21 (1)			{−1.00	−1.27	−1.52}[c]	

[a] Concentrations of electroactive species are in the range 0.1 → 5 mm; $E_{1/2}$ *vs.* sce; DME employed as working electrode: numbers in parentheses are number of electrons for particular electrode process. [b] Total sum of electrons involved in the reduction processes. [c] Non-integral values of n observed.

undergoes two Nernstian one-electron reductions in DMF at −1.23 and −1.52 V *vs.* the normal calomel electrode, nce, to produce the dianion, $[A]^{2-}$. The dianion, an aromatic entity with 18 π-electrons, which tends to adopt a planar structure, enjoys much more stabilization by electron delocalization than does the parent [16]annulene.

For a number of years we have been engaged in the study[8] of the metal complexes of a tetraaza[16]annulene, namely, tetrabenzo[*b*,*f*,*j*,*n*][1,5,9,13]tetraazacyclohexadecine (abbreviated TAAB, structure II). Note that structures I and II differ in the location and nature of

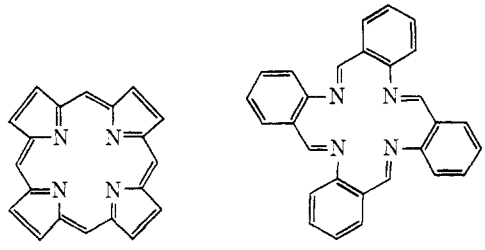

I

II

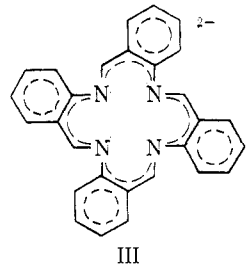

III

their fused rings but that they contain the same alternating unsaturated inner-most 16-membered ring. Further, the two-electron reduction of TAAB should produce an aromatic porphyrin-like dianion (structure III). Just as many metal complexes of the porphyrin ring are stable under ambient conditions so are many of those of TAAB. The obvious diverse stabilities of the dianion on the one hand and of the neutral ligand on the other must result from the different kinds of fused rings in the two frameworks.

Although the annulene form (oxidized) of the complexes, derived from ligands having the framework in structure II, is most stable, we report here evidence for the formation of the aromatic (porphyrin-like) dianion by electrochemical reduction. Still more important, we have succeeded in the isolation and characterization of a number of cobalt, copper, and nickel complexes of this important new ligand. The unique electrochemistry exhibited by the reduced complexes of cobalt serves to further confirm the formulation of the ligand in these complexes as the aromatic dianion, $TAAB^{2-}$.

(8) G. A. Melson and D. H. Busch, *J. Amer. Chem. Soc.*, 86, 4830, 4834 (1964); V. Katovic, L. T. Taylor, and D. H. Busch, *ibid.*, 91, 2122 (1969).

Results and Discussion

The electrochemical properties of $Co^{II}(TAAB)^{2+}$, $Ni(TAAB)^{2+}$, and $Cu(TAAB)^{2+}$, as well as the nickel and copper complexes with the related ligands of structures IV, $[(TAAB)(OMe)_2]^{2-}$, and V, H_8TAAB,

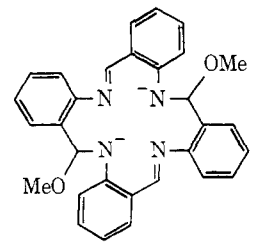

IV

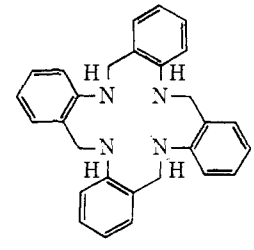

V

were studied in the protic solvent CH_3OH (Table I) and in the aprotic solvent acetonitrile (Table II). The broad range of available potentials together with the absence of complicating protonation reactions were factors in choosing acetonitrile as the second solvent for the study of these systems. The contrasting behavior in the protic and aprotic media proved to be illuminating.

Nickel Complexes. The polarogram for $Ni(TAAB)^{2+}$ in methanol (using potassium chloride as the supporting electrolyte and a saturated calomel electrode (sce) as the reference electrode (Figure 1)) displays two well-defined one-electron reduction waves, corresponding *formally* to reduction to Ni(I) and to Ni(0), respectively. Cyclic voltammetric studies show the first reduction wave to be non-Nernstian, while the second wave displays nearly Nernstian behavior. When Et_4NClO_4 supporting electrolyte is used, both processes display nearly Nernstian waves. At higher negative potentials an irreversible eight-electron process occurs, presumably coupled with simultaneous protonation processes ($E_{1/2}$ = −1.57 V *vs.* sce). The total number of electron

Table II. Electrochemical Data for the TAAB Complexes in Acetonitrile[a]

Complex	$E_{1/2}$	Complex	$E_{1/2}$
$NiTAAB(ClO_4)_2$	+1.24 (−1)[b]	$CoTAAB(ClO_4)_2$	+0.51 (−1)
	−0.64 (1)		−0.85 (1)
	−0.93 (1)		−1.22 (1)
	−2.4 (1)		−1.85 (1)
$NiTAABClO_4$	−0.64 (−1)	$CoTAABClO_4$	+0.51 (−1)
	−0.93 (1)		+0.25 (−1)
NiTAAB			−1.02 (1)[c]
	−0.64 (−1)		−1.76 (1)
	−0.93 (−1)		
$CuTAAB(ClO_4)_2$	+1.23 (−1)	$CoTAAB\cdot CH_3CN$[d]	+0.50 (−1)
	−0.23 (1)		+0.28 (−1)
	−1.49 (1)		−0.92 (−1)
			−1.80 (1)

[a] $E_{1/2}$ *vs.* $Ag|AgNO_3$ (0.1 *M*); 5×10^{-2} *M* Et_4NClO_4 supporting electrolyte; rotating platinum electrode used as working electrode. [b] Numbers in parentheses refer to number of electrons transferred. [c] Quasi-reversible with cyclic voltammetric ΔE_p = 140 mV. [d] This complex also exhibits waves at −0.15 and −0.57 V which are only 34% of the other wave heights.

and proton additions is sufficient to hydrogenate all four azomethine linkages in the TAAB macrocycle forming H_8TAAB (V) and to reduce the Ni(II) to Ni(0).

The nickel complex of $[(TAAB)(OMe)_2]^{2-}$ [9] (IV) contains only two C=N functions and has a −2 charge. Its polarogram in methanol displays a non-Nernstian one-electron wave at $E_{1/2}$ = −0.50 V *vs.* sce, followed by a five-electron reduction process at −1.54 V. Despite structural differences, the total number of reduction equivalents is again sufficient to both produce Ni^0 and completely hydrogenate all available azomethine groups.

The complex $Ni(H_8TAAB)^{2+}$, where H_8TAAB is the fully saturated macrocycle (structure V), gives a simple two-electron wave and no multi-electron-ligand hydrogenation wave, in full accord with expectations (Figure 1). This nearly reversible ($E_{3/4} - E_{1/4}$ = −26 mV; theoretical, −29 mV) polarographic reduction wave with an $E_{1/2}$ of −0.97 V *vs.* sce is similar to waves observed for $Ni(2,2'\text{-bipy})_3^{2+}$.[10] However, cyclic voltammetric studies at a hanging mercury drop reveal that $Ni(H_8TAAB)^{2+}$ shows a non-Nernstian but chemically reversible behavior; *i.e.*, i_{pc}/i_{pa} = 0.98 and $\Delta = E_{pa} - E_{pc}$ = 170 mV. The polarograms of Ni(TAAB)-$(OMe)_2$ and $Ni(H_8TAAB)^{2+}$ are depicted in Figure 1 together with that of $Ni(TAAB)^{2+}$ to illustrate the differences in their behavior in methanol. The electrochemical data for $Ni^{II}(TAAB)^{2+}$ and its derivatives are given in Table I.

Acetonitrile is an aprotic solvent which may be used over a broad potential region extending to −2.8 V *vs.* sce.[11] In this solvent, the nickel complexes undergo reductions similar to those observed in methanol for those electrode processes formally involving the metal ion. However, very cathodic electrode processes involving hydrogenation of the ligand system are entirely different, quite obviously because of the absence of a source of protons. The electrochemical data obtained in acetonitrile are shown in Table II. All potentials are measured against the electrode Ag wire|0.1 *M* Ag^+–acetonitrile. At +1.24 V, $Ni(TAAB)^{2+}$ shows a quasi-Nernstian one-electron oxidation wave, Ni(II) → Ni(III), with $E_{3/4} - E_{1/4}$ = +67 mV. In the cathodic region three separate electrode processes occur producing substances, formally corresponding to Ni(I), Ni(0), and Ni(−I), respectively. The first two nearly Nernstian waves have $E_{3/4} - E_{1/4}$ values of −62 and −66 mV, while the third reduction has a value of 42 mV and is far from Nernstian in behavior. The Nernstian behavior of the first two reductions has been confirmed by cyclic voltammetry at the Pt-microsphere electrode (Figure 2). Controlled-potential coulometry of $Ni(TAAB)(BF_4)_2$ in acetonitrile at −0.75 V *vs.* Ag wire|0.1 *M* $AgNO_3$–CH_3CN yielded duplicate *n* values of 1.00 and 1.04.

Controlled-potential oxidation of $Ni(TAAB)^{2+}$ in acetonitrile at +1.40 V *vs.* Ag wire|0.1 *M* $AgNO_3$–CH_3CN produces solutions of $Ni(TAAB)^{3+}$. After complete oxidation the color of the solution turns from red to dark green. Application of controlled-potential

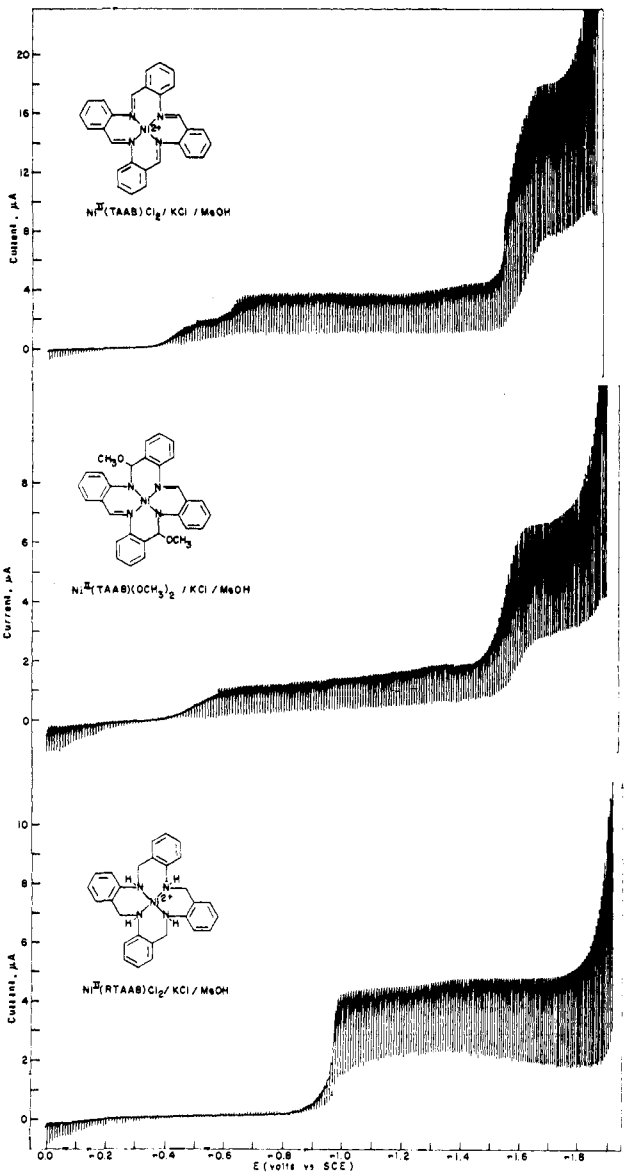

Figure 1. Polarograms of $Ni(TAAB)^{2+}$, $Ni(TAAB)(OCH_3)_2$, and $Ni(H_8TAAB)^{2+}$ in CH_3OH.

(9) L. T. Taylor, F. L. Urbach, and D. H. Busch, *J. Amer. Chem. Soc.*, 91, 1072 (1969).
(10) A. A. Vlcek, *Z. Elektrochem.*, 61, 1014 (1957).
(11) I. M. Kolthoff and J. F. Coetzee, *J. Amer. Chem. Soc.*, 79, 870 (1957).

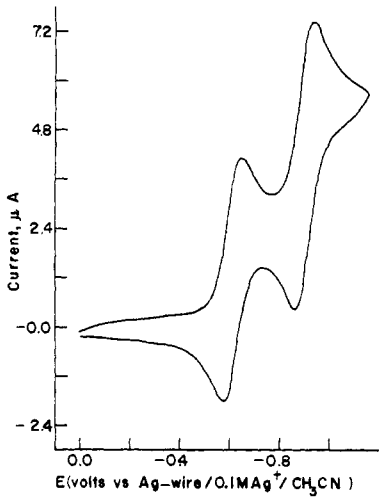

Figure 2. Cyclic voltammogram of $Ni(TAAB)(BF_4)_2$ in acetonitrile. The scan rate is 0.033 V/sec.

coulometry here yielded an n value of 0.94 indicating a single one-electron oxidation.

Copper Complexes. The pattern of electrochemical behavior of the copper complexes is very similar to that of nickel. In methanol (Table I) $Cu^{II}(TAAB)^{2}$ displays a single one-electron reduction process at the rotating Pt electrode, *i.e.*, Cu(II) → Cu(I). At more negative potentials, several broad, ill-defined waves appear. These waves are thought to derive from complicated hydrogenation processes and are so broadened that the final diffusion currents are difficult to measure accurately. The limiting current for each process formally involving the metal center is diffusion controlled; *i.e.*, a plot of i_d *vs.* $h_{1/2(corr)}$ gives a straight line.

Controlled-potential coulometry of the $Cu(TAAB)^{2+}$ reduction process resulted in n values of 1.02 and 1.04 (at −0.15 V *vs.* sce).

$[Cu(TAAB)(OMe)_2]$,[12] the complex with two imine functions, undergoes a one-electron Nernstian Cu(II) → Cu(I) reduction at more negative potentials (−0.38 V more cathodic) than the parent $[Cu(TAAB)]^{2+}$ complex. At still more negative potentials the two imine functions are hydrogenated by complicated mechanisms over a potential range of 0.7 V.

In acetonitrile $Cu(TAAB)^{2+}$ undergoes two reduction processes, formally producing Cu(I) and Cu(0) at $E_{1/2}$'s of −0.23 and −1.49 V *vs.* Ag wire|0.1 *M* Ag^+–CH_3CN, respectively (+0.13 and −1.13 V *vs.* sce). Cyclic voltammetric study indicated the quasi-Nernstian nature of both processes with $\Delta = E_{pa} = E_{pc}$ of 65 and 79 mV (E_{pa} and E_{pc} are the anodic and cathodic peak potentials, respectively) and $i_{pc}/i_{pa} = 0.93$ and 1.08 for the first and second couple, respectively (i_{pc}/i_{pa} is the ratio of the forward peak current to reverse peak current). In agreement with the nickel case, $Cu(TAAB)^{2+}$ does not undergo hydrogenation in acetonitrile. The pertinent redox data for $Cu(TAAB)^{2+}$ in acetonitrile are given in Table II.

Cobalt Complexes. The electrochemistry of $Co(TAAB)^{2+}$ was studied both in the solvent methanol and in the aprotic solvent acetonitrile. The voltammetric data in MeOH, summarized in Table I, revealed the occurrence of three successive one-electron reductions followed by a complicated multielectron process ($E_{1/2}(4)$ through $E_{1/2}(6)$). The hydrogenation of the four imine functions at the dme in methanol solution ($E_{1/2}(4)$ through $E_{1/2}(6)$, Table I) shows a strong dependence on solvent and background electrolyte. An eight-electron change is required to hydrogenate all four azomethine linkages (structure V) and the simplest behavior observed corresponds to an electron change of that number.

While the hydrogenation processes show a considerable sensitivity to the nature of the electrolyte in CH_3OH solutions, the less cathodic reductions at dme display nicely reproducible $E_{1/2}$ values (regardless of X in $Co^{II}(TAAB)X_2$) in the presence of a given electrolyte. Thus for Et_4NClO_4 supporting electrolyte they occur at −0.54 to −0.55 V, −0.87 to −0.90 V, and −1.05 to −1.07 V. The data generally show a decreasing potential range of stability for the products of successive reduction processes.[13]

In accord with expectations, no electrode process attributable to the hydrogenation of the azomethine groups occurs in purified acetonitrile. It is worth mentioning that such "ligand double bond reductions" have been claimed for other systems in acetonitrile.[14] The transfer of one electron into a vacant antibonding orbital is expected, but this product should not undergo protonation or further reduction in an aprotic solvent such as acetonitrile.

Rpe voltammograms of $Co^{II}(TAAB)(ClO_4)_2$ in acetonitrile, using Et_4NClO_4 as the supporting electrolyte and Ag wire|0.1 *M* $AgNO_3$–CH_3CN as the reference electrode, display three consecutive one-electron reduction waves (Table II). These processes reduce the *formal* oxidation state of the cobalt stepwise to a Co(−I) d^{10} configuration, paralleling the behavior in methanol. As is the case in methanol, the reduction of Co(II) to Co(I) is a Nernstian electrode process. This result is most striking and is a matter of considerable significance to later discussions.

The Annulene–Aromatic Ligand Transformation. A close look at the reduction process of the family of TAAB complexes in acetonitrile assigned *formally* to the metal center discloses the most dramatic characteristic of these reductions. It appears that an electron saturation effect occurs when the metal ion achieves the d^{10} configuration within the TAAB complex by accepting one electron in the case of the $Cu(TAAB)^{2+}$, two electrons in the case of the $Ni(TAAB)^{2+}$, and three electrons in the case of $Co(TAAB)^{2+}$. Thus we conclude that additional stability is achieved for those

(12) V. Katovic, L. T. Taylor, and D. H. Busch, *Inorg. Chem.*, **10**, 458 (1971).

(13) The rpe voltammograms of $Co^{III}(TAAB)(NO_3)_3$ in methanol display an interesting behavior not reported in Table I. Voltammograms run *immediately* after dissolving the compound show a non-Nernstian Co(III)–Co(II) reduction at ~+0.61 V *vs.* sce. The second reduction, Co(II) → Co(I), occurs at −0.55 V and the third process at −0.92 V. Only the first wave need concern us at this point. As time proceeds, the first half-wave potential becomes more negative and eventually becomes constant at $E_{1/2} = +0.51$ V. The other half-wave potentials do not shift with time. However, there is an increase in the current height of the Co(II) → Co(I) reduction wave, while the height of the Co(III) → Co(II) wave decreases. Eventually the Co(III) → Co(II) wave completely vanishes. This is accompanied by a gradual change of the initial orange-brown color to green. This behavior indicates the occurrence of two processes. The first is probably solvent displacement of the coordinated anion while the second clearly involves reduction of the cobalt(III) complex by a chemical reaction in the bulk of the solution. The reduction of $Co^{III}(TAAB)(NO_3)_3$ to $Co^{II}(TAAB)(NO_3)_2$ in methanol is accelerated by heating the solution.

(14) D. C. Olson and J. Vasilevskis, *Inorg. Chem.*, 8, 1516 (1969).

particular reduced ligand–metal ion species where the sum of the ligand π-electrons plus the number of metal ion d electrons is 42. The idealized electron accounting associated with the electrochemical reduction of the divalent $Cu(TAAB)^{2+}$, $Ni(TAAB)^{2+}$, and $Co(TAAB)^{2+}$ complexes is summarized in Table III.

Table III. Idealized Electron Accounting for Final Reduction Products of $M^{II}(TAAB)^{2+}$

Complex	No. of electrons: d electrons M^{II}	π-electrons, TAAB	Electrode	Total
$Cu^{II}(TAAB)^{2+}$	9	32	1	42
$Ni^{II}(TAAB)^{2+}$	8	32	2	42
$Co^{II}(TAAB)^{2+}$	7	32	3	42

It is obvious that one might formulate the stabilized reduction products $Cu(TAAB)^{+}$ $Ni(TAAB)^{0}$, and $[Co(TAAB)]^{-}$ in either of two extreme ways. First, if one merely assumes that the added electrons are associated exclusively with the metal center, these reduction products are assigned d^{10} electronic configurations, $[Ni^{0}(TAAB)]^{0}$, $[Cu^{I}(TAAB)]^{+}$ and $[Co^{-I}(TAAB)]^{-}$.[11] However, it is not the d^{10} configuration that is favored by square-planar coordination, but rather a d^{8} configuration. Hawkinson and Fleischer's[15] crystallographic studies have shown that the TAAB macrocycle adopts a square-planar coordination geometry. Consequently, the ligand TAAB should indeed stabilize a d^{8} metal ion configuration.

The second extreme formulation involves assignment of the added electrons to the ligand. As mentioned earlier, TAAB is an analog of the nonaromatic, alternating hydrocarbon, tetrabenzo[16]annulene, structure VI, which is derived from [16]annulene.[6]

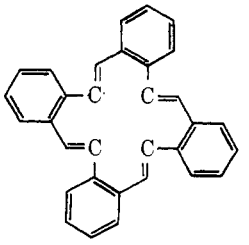

VI

Consequently, TAAB itself with 32 π-electrons is not expected to exhibit the extreme electron delocalization associated with aromaticity; however, the addition of two electrons to its weakly conjugated π-system should produce a Hückel aromatic analog to the porphyrin dianion ring. We have already established that the system has a special ability to stabilize reduced systems wherein the sum of the number of metal ion d electrons plus the π-electrons reaches 42. This amounts to the eight d electrons needed to fill the four low-lying d orbitals on the metal ion in D_{4h} (or related) symmetry and a ligand π-electron system of 34 electrons. Thus, the ligand TAAB has been effectively reduced to the aromatic dianion $TAAB^{2-}$. Of course, though the real system more nearly approaches the second of the two extreme descriptions, the actual molecular orbitals

(15) S. W. Hawkinson and E. B. Fleischer, *Inorg. Chem.*, 8, 2402 (1969).

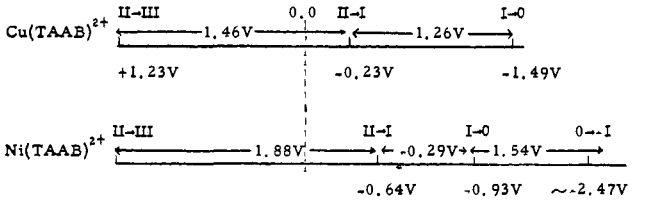

Figure 3. Differences in $E_{1/2}$ for electrode processes involving $Cu(TAAB)^{2+}$ and $Ni(TAAB)^{2+}$ in CH_3CN.

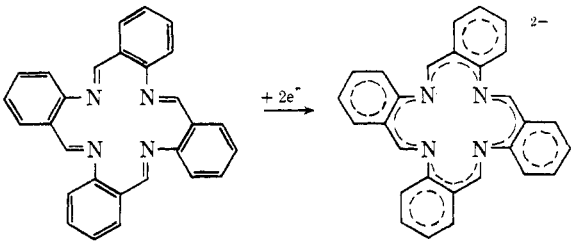

will reflect strong mixing of the metal ion and ligand π orbitals. Insofar as the assignment of oxidation states is a useful exercise in systems of this class, it is preferable to utilize the second model presented here. Thus the ultimate reduction products are formulated as $[Cu^{III}(TAAB^{2-})]^{+}$, $[Ni^{II}(TAAB^{2-})]^{0}$, and $[Co^{I}(TAAB^{2-})]^{-}$. Note that the reduction product derived from the copper(II) complex is assigned an increased oxidation state. Presumably, this is made possible by the formation of an aromatic molecule containing 34 π-electrons, which because of its associated resonance energy is strongly favored over the nonaromatic TAAB.

It is not clear whether these stepwise one-electron reductions occur first at the metal ion followed by rearrangement of the product *via* an intramolecular oxidation–reduction process to produce the reduced ligand or whether the reductions occur directly at the ligand, as inferred by Wolberg and Manassen[1] for the converse case, the oxidation of the porphyrins. We confront this matter more directly later in the text in the case of $Co(TAAB)^{2+}$.

The electrochemical behavior of the parent macrocyclic complexes $Ni(TAAB)^{2+}$ and $Cu(TAAB)^{2+}$ is easily rationalized in terms of the structural model we have proposed (Figure 3). It is immediately obvious that $[Cu^{III}(TAAB^{2-})]^{+}$ is very stable toward reduction and oxidation over a broad range of potentials. This is consistent with its having the ideal numbers of both ligand and metal ion electrons. The situation is somewhat different for $Ni(TAAB)^{2+}$. Three limiting formulations must be considered for its first reduction product: $[Ni^{I}(TAAB)]^{+}$, $[Ni^{II}(TAAB^{-})]^{+}$, $[Ni^{III}(TAAB^{2-})]^{+}$. This electrochemical product is unstable to both oxidation and reduction; that is it exists in equilibrium with the electrode over a very limited range of potentials (*ca.* -0.6 to -0.9 V). If one adopts the viewpoint that this substance should be formulated as $[Ni^{III}(TAAB^{2-})]^{+}$, then facile reduction of d^{7} Ni^{III} to d^{8} Ni^{II} is expected. We present esr evidence consistent with this view in a later section.

Based on these considerations, it would be expected that $[Ni^{II}(TAAB^{2-})]^{0}$ would not be easily susceptible to further reduction. The next (third) electron, which is accepted by the previously reduced neutral molecule, goes into an antibonding π-orbital which is of high energy, thus making the reduction to $[Ni^{I}(TAAB^{2-})]^{-}$

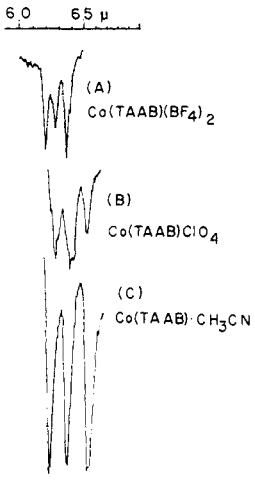

Figure 4. Infrared spectra of the cobalt complexes in the 1500–1650-cm^{-1} region.

difficult. Complexes of formally uninegative nickel have been shown to exist by electrochemical means.[16] $[Ni(2,2'\text{-bipy})_3]^-$ is formed in CH_3CN by a one-electron reduction of $[Ni(2,2'\text{-bipy})_3]^0$ at the dme.

In order to examine the reduced complexes of TAAB more fully, we now turn to their synthesis and detailed characterization.

Synthesis and Characterization of the New Complexes. Reductions of the parent macrocyclic complexes at controlled potential in acetonitrile on the plateaus of the appropriate reduction steps give new complexes containing formally univalent and zerovalent metal ions. In this manner, we have prepared Ni(TAAB)-ClO_4, Ni(TAAB), Cu(TAAB)PF_6, Co(TAAB)ClO_4, and Co(TAAB)·CH_3CN. These compounds have been characterized by elemental analysis and a number of physical measurements. Their analytical data are given in the Experimental Section. The results of physical measurements on these reduced compounds imply quite strongly that they should be considered to be derived from $TAAB^{2-}$, structure III, rather than from TAAB itself.

The infrared spectral data for Ni(TAAB)$(BF_4)_2$, Ni(TAAB)ClO_4, Ni(TAAB), and Cu(TAAB)PF_6 are listed in Table IV. The spectra for the family of cobalt complexes are shown in Figure 4.

Table IV. Infrared Spectral Bands for the Ni- and Cu-TAAB Derivatives

Assignment	Ni(TAAB)-$(BF_4)_2$	Ni(TAAB)-ClO_4	Ni(TAAB)	Cu(TAAB)-PF_6
C_6, ring I	1610 vs	1615 m	1615 m	?
C_6, ring II	1590 s	1593 m	1594 w	1595 m
C=N	1568 vs	1569 w	1575 m	1567 m
		1545 w		1555 m
		1515 m		1534 s
C_6, ring III	1492 m	1495 w	1494 m	1480 s
C_6, ring IV	1440 m		1455 s	1435 s

The infrared spectra of $M(TAAB)^{2+}$ complexes, where M = Cu(II), Ni(II), Co(II), Co(III), Fe(III), Pd(II), and Zn(II), are very similar. They all contain three very strong absorption bands in the region 1650–1550 cm^{-1}. These are characteristic of the presence of the TAAB ligand. The bands at 1610 and 1590 cm^{-1} are two of the ring modes of the benzene rings, while the band at 1568 cm^{-1} is attributed, on the basis of hydrogenation experiments, principally to the C=N stretching mode.[17] However, the so-called "reduced compounds," Ni(TAAB)ClO_4, Ni(TAAB), Cu(TAAB)-PF_6, Co(TAAB)ClO_4, and Co(TAAB)·CH_3CN, display considerably different vibrational spectral behavior. This is most obvious in the region where C=N and C=C bands occur (1650–1500 cm^{-1}). Considering the complexes of cobalt as an example (Figure 4), the three bands in $Co^{II}(TAAB)(ClO_4)_2$ are assigned as follows[18] (following the assignments of ref 19): those at 1608 and 1594 cm^{-1} are the ring modes of the benzene rings and the band at 1568 cm^{-1} is due principally to the C=N stretching mode. In the reduced products, all the bands are found at lower energies (1594, 1567, and 1531 cm^{-1} for Co(TAAB)ClO_4 and 1598, 1566, and 1525 for Co(TAAB)·CH_3CN). This is consistent with the increased negative charge carried by the ligand $TAAB^{2-}$ and the more extensive delocalization between the C–N fragment and the rest of the aromatic system.

The infrared spectra of the reduction products also clearly show the presence of perchlorate and acetonitrile in the respective complexes. The acetonitrile in the complex $Co^{II}(TAAB^{2-})CH_3CN$ is probably not coordinated to the metal since $\nu_{C\equiv N}$ occurs at 2243 cm^{-1} in the infrared spectrum. This is comparable with the position observed for acetonitrile of crystallization while higher frequencies (over 2290 cm^{-1}) are expected for coordinated acetonitrile.[20] Parallel results are found for the reduced complexes of copper and nickel. For example in the region 1650–1500 cm^{-1}, Cu(TAAB)-PF_6, Ni(TAAB)ClO_4, and NiTAAB display several low intensity absorption bands in contrast to the three strong bands found in the spectrum of the parent Ni(TAAB)$(BF_4)_2$ and Cu(TAAB)$(PF_6)_2$. In addition, the formulated stoichiometries of these reduced compounds are confirmed by the presence or absence of the appropriate counteranion in the infrared spectrum.

The positions of the C=N stretching bands in the reduced complexes are comparable with the frequencies of the corresponding groups in the spectra of the nickel[18] and copper complexes[21] of the so-called "solvolyzed" TAAB, in which two anionic bases (R^-) have been added to the TAAB ligand, structure IV. This result is as would be expected, since each negative charge in $[TAABR_2]^{2-}$ is delocalized over half of the molecule in a manner, which, though different, is analogous to that associated with the negative charges in $TAAB^{2-}$.

Magnetic susceptibility measurements show that Cu(TAAB)PF_6, Ni(TAAB), and Co(TAAB)ClO_4 are low spin while Ni(TAAB)ClO_4 is paramagnetic with one unpaired electron (μ_{eff} = 1.94 BM). The complex Co(TAAB)·CH_3CN has μ_{eff} = 2.84, significantly higher than the spin-only value for one electron. This

(16) N. Tanaka and Y. Sato, *Inorg. Nucl. Chem. Lett.*, **9**, 487 (1968).

(17) L. T. Taylor, F. L. Urbach, V. Katovic, W. White, and D. H. Busch, *Inorg. Chem.*, **11**, 479 (1972).

(18) L. T. Taylor, F. L. Urbach, and D. H. Busch, *J. Amer. Chem. Soc.*, **91**, 1072 (1969).

(19) S. C. Cummings and D. H. Busch, *Inorg. Chem.*, **10**, 1220 (1971).

(20) K. Farmery and D. H. Busch, unpublished results.

(21) L. T. Taylor, F. L. Urbach, V. Katovic, and D. H. Busch, unpublished results.

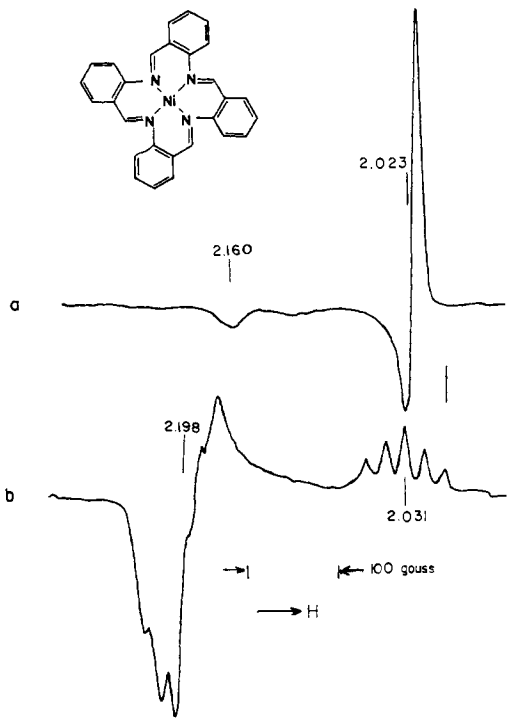

Figure 5. Electron spin resonance spectra of $Ni^{III}(TAAB^{2-})^{+}$ and $Ni^{III}(TAAB)^{3+}$.

value is reasonable for the formulation $Co^{II}(TAAB^{2-})$ since relatively large values are not uncommon for low spin d^7 in planar complexes. The most relevant case is that of β-Co(phthalocyanine) whose moment is 2.73 BM.[22] This high value has been explained[22,23] on the basis of esr measurements, in terms of a high orbital contribution from the odd electron in the d_{z^2} orbital.

In elucidating the proposed electronic structures, the parameters derived from esr studies on $Ni(TAAB)^{+}$ are helpful (Table V and Figure 5). Clearly the spectrum is not that of a radical anion so the structure $[Ni^{II}(TAAB^{-})]^{+}$ can be disregarded. Three likely structures remain: four-coordinate planar nickel(I) in $Ni^{I}(TAAB)^{+}$, four-coordinate planar nickel(III) in $Ni^{III}(TAAB^{2-})^{+}$, and six-coordinate tetragonal nickel(III) in $[Ni^{III}(TAAB^{2-})(solvent)_2]^{+}$. We can confidently eliminate the latter structure because it places the unpaired electron in d_{z^2} and theory[24] predicts $g_{\perp} > g_{\parallel}$ whereas we observe the opposite result (Table V and Figure 5). In the case of the oxidation product $Ni^{III}(TAAB)(CH_3CN)_2^{3+}$, these expectations are fulfilled (Table V and Figure 5). Further, studies on a broad array of tetragonal Ni(III) complexes, conducted under precisely similar conditions (77°K, frozen acetonitrile), all show a similar superhyperfine splitting pattern of the signal by the axially coordinated solvent molecules.[25] This is not observed in the case of the reduction product while it does occur for the oxidation product.

Table V. Esr Data for $Ni(TAAB)^{+}$ and Related Complexes

Complex	$g_{\perp}$	$g_{\parallel}$	Formulation
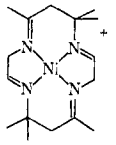	2.053	2.195	Ni(I), d^9
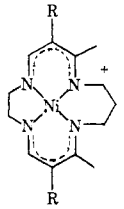	2.012	2.144	Square-planar Ni(III), d^7
$Ni(TAAB)(CH_3CN)_2^{3+}$	2.197 (A = 17 G)	2.031 (A = 21.6 G)	Tetragonal, six-coordinate Ni(III)
$Ni(TAAB)^{+}$	2.023	2.160	(See text)

It is more difficult to distinguish between the two remaining possibilities for, as the comparison given in Table V shows, the $g_{\perp}$ and $g_{\parallel}$ for $Ni(TAAB)^{+}$ fall between those observed for related square-planar Ni(I) and Ni(III) complexes. The results of studies of many Ni(I) and Ni(III) macrocyclic complexes[25] allow us to apply the expression $g_{\parallel} = 2 - (8\lambda/\Delta)$ to this problem. This position of TAAB in a spectrochemical series for macrocyclic ligands for Co(III) and Ni(II) should provide a reasonable estimate of the relative ligand field toward Ni(I).[26] We also assume λ to be about the same for a series of macrocyclic ligands containing only nitrogen donors in nonaromatic ligands. On this basis we would predict $g_{\parallel}$ to be about 2.24 for $Ni^{I}(TAAB)^{+}$. In order to arrive at the experimental value of 2.16, we must assume that λ is much smaller for the TAAB complex than for the other nickel(I) derivatives. No such paradox arises if we assume the complex to be square planar $Ni^{III}(TAAB^{2-})^{+}$. Consequently, we conclude that our esr data are consistent with the suggestion that the product of one-electron reduction of $Ni^{II}TAAB^{2+}$ actually contains oxidized metal ion (Ni(III)) but two-electron reduced ligand $TAAB^{2-}$.

The electronic spectra of the one-electron reduction products consist of a number of intense bands ranging from the near-infrared region into the ultraviolet. Their high molar absorptivities identify them as ligand transitions or metal–ligand charge transfer processes. The spectra of $Cu(TAAB)^{+}$ and $Ni(TAAB)^{+}$ are summarized in Table VI. The spectrum of $Cu(TAAB)PF_6$,

Table VI. Electronic Spectra of $Ni(TAAB)^{+}$ and $Cu(TAAB)^{+}$

Complex	λ_{max}, cm^{-1}	ϵ_{max}
$Cu(TAAB)^{+}$	14,180	6,400
	27,780 (sh)	14,900
	31,056	20,500
$Ni(TAAB)^{+}$	10,100	7,000
	18,870	1,700
	22,727	4,560
	26,881	16,380
	32,050	31,200

(22) B. N. Figgis and R. S. Nyholm, *J. Chem. Soc.*, 338 (1959).
(23) J. M. Assour and W. K. Kahn, *J. Amer. Chem. Soc.*, 87, 207 (1965).
(24) A. H. Maki, N. Edelstein, A. Davison, and R. H. Holm, *J. Amer. Chem. Soc.*, 86, 4580 (1964).
(25) E. S. Gore, F. V. Lovecchio, and D. H. Busch, unpublished results.
(26) D. H. Busch, *Helv. Chim. Acta, Werner Commemoration Volume*, 174 (1967); C. R. Sperati, Thesis, Ohio State University, Columbus, Ohio, 1971.

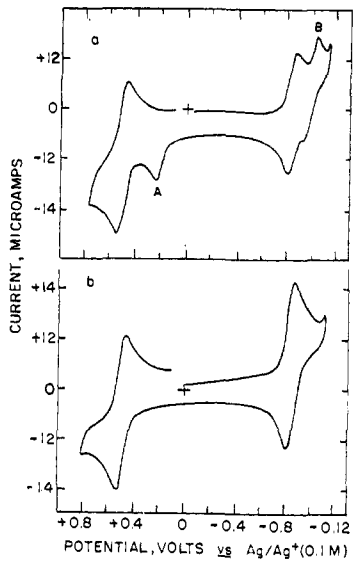

Figure 6. (a) Cyclic voltammogram of $Co^{II}(TAAB)^{2+}$ in acetonitrile solution at a platinum wire electrode, after partial electrolysis at −0.95 V. (A and B show the appearance of the waves of $Co^{III}(TAAB^{2-})^{+}$.) (b) Cyclic voltammogram of the oxidation and first reduction process of $Co^{II}(TAAB)(ClO_4)_2$ in acetonitrile solution.

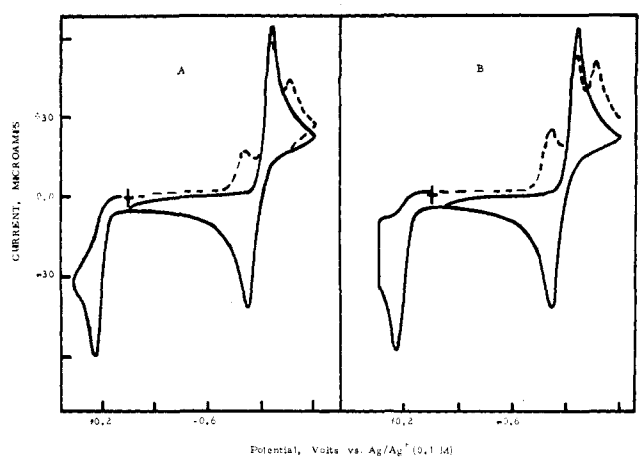

Figure 7. Multiple scan cyclic voltammograms of $Co^{III}(TAAB^{2-})ClO_4$ in acetonitrile solution at a platinum electrode surface. Solid lines are curves obtained after first potential sweep cycle. Sweep started cathodically a 0.0 V. Dotted lines show appearance of new waves on second and subsequent sweep cycles in both curves A and B. Curve B shows increased buildup of $Co(TAAB)^{2+}$ as a result of holding the potential at +0.3 V (for ~45 sec).

as a solid and in methanol solution, is reported elsewhere.[12] The electronic spectrum of $Co(TAAB)^{+}$ will be discussed separately below.

Electrochemistry of the New Complexes. The assignment of structure III ($TAAB^{2-}$) to the ligand in the products of electrochemical reduction of $M^{II}(TAAB)^{2+}$ again emphasizes the relationship between the aromatic dianion ligands, such as $TAAB^{2-}$ or porphyrin, and their corresponding two-electron oxidation products, *i.e.*, TAAB and the annulene of structure I. The electrochemical behavior of the reduction products in acetonitrile, $Co^{III}(TAAB^{2-})ClO_4$ and $Co^{II}(TAAB^{2-})CH_3CN$ (Table II), provides strong additional evidence for these concepts. We infer that formation of the aromatic dianion $TAAB^{2-}$ from TAAB requires molecular rearrangement, since X-ray studies[15] on $Ni(TAAB)^{2+}$ derivatives show much less planarity in the ligand than would be anticipated for an aromatic dianion such as $TAAB^{2-}$. The coupling of a significant molecular and electronic rearrangement to one or more electrode processes might be detected in favorable cases.

We have stated above that the first one-electron reduction process for $Co^{II}(TAAB)^{2+}$ (or the second for $Co^{III}(TAAB)^{3+}$) is Nernstian in character. The process occurs at rpe at about -0.85 ± 0.02 V (depending on solution conditions) *vs.* Agwire|0.1 *M* $AgNO_3$–CH_3CN. In the simplest of circumstances, the one-electron reduction product, isolated after cpe at −0.95 V, should exhibit two oxidation waves, the first one corresponding to

$$Co^{I}(TAAB)^{+} \underset{+e^-}{\overset{-e^-}{\rightleftharpoons}} Co^{II}(TAAB)^{2+}$$

at $E_{1/2} = -0.85$ V and a second wave corresponding to

$$Co^{II}(TAAB)^{2+} \underset{+e^-}{\overset{-e^-}{\rightleftharpoons}} Co^{III}(TAAB)^{3+}$$

at $E_{1/2} = +0.51$ V. As indicated in Table II, this most certainly is *not* the case. The first oxidation wave of the substance of composition $Co(TAAB)ClO_4$ is an irreversible one, appearing at +0.25 V, followed by a reversible oxidation at $E_{1/2} = +0.51$ V. Furthermore, a reduction wave occurs at $E_{1/2} = 1.02$ V. The processes at +0.25 and −1.02 V do not appear in the redox behavior of $Co^{II}(TAAB)(ClO_4)_2$. The nature of these curves, which will be more fully developed below, is consistent with the conclusion that the addition of one electron to the cobalt(II) complex of TAAB yields a relatively unstable intermediate which is the reduced partner of the couple given below

$$Co^{II}(TAAB)^{2+} \underset{-e^-}{\overset{+e^-}{\rightleftharpoons}} Co^{I}(TAAB)^{+}$$

The product of this reaction contains cobalt(I) and the original annulene-like ligand. This product is metastable with respect to a product of intramolecular oxidation–reduction, $Co^{III}(TAAB^{2-})^{+}$. The latter is formed by an internal redox reaction wherein two electrons are transferred from orbitals primarily localized on the metal ion to orbitals primarily localized on the ligand. The Frank–Condon principle requires the prior rearrangement of the ligand skeleton to that commensurate with the relatively planar ligand dianion produced by electron transfer. The rearrangement reaction is

$$Co^{I}(TAAB)^{+} \longrightarrow Co^{III}(TAAB^{2-})^{+}$$

The product isolated in the solid state contains the rearranged cation and the electrochemistry of the solutions of this product is therefore that of $Co^{III}(TAAB^{2-})^{+}$. The fact that the first oxidation wave for this material occurs at a much more anodic potential than does the corresponding wave for the unrearranged $Co^{I}(TAAB)^{+}$ is consistent with the expected enhancement of stability associated with the aromatic nature of the ligand in the rearranged complex, $Co^{III}(TAAB^{2-})^{+}$.[6]

An excellent example of this type of behavior can be found[27] from the redox characteristics of derivatives of 2-methoxyazocine, which undergo a two-electron re-

(27) L. B. Anderson, J. F. Hansen, T. Kakihana, and L. A. Paquette, *J. Amer. Chem. Soc.*, **91**, 196 (1969).

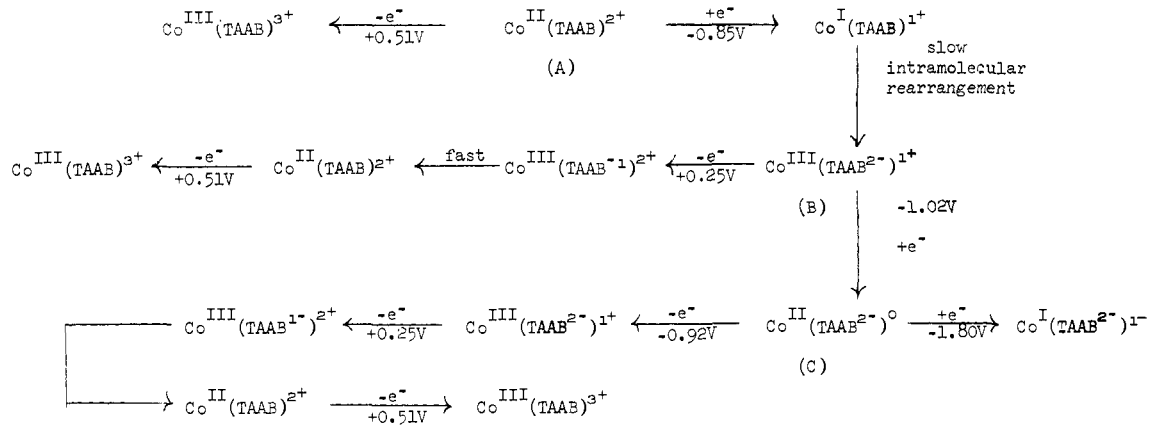

Figure 8. Oxidation–reduction processes of $Co^{II}(TAAB)^{2+}$ and its derivatives as observed in acetonitrile solution.

duction to form an aromatic dianion. The stability of this dianion is such that its reoxidation does not occur until a potential is reached which is ~0.8 V more anodic than the reduction potential of the parent azocine.

Further support for this point of view is found in the behavior of the product of two-electron reduction, $Co(TAAB)\cdot CH_3CN$, formulated as $Co^{II}(TAAB^{2-})\cdot CH_3CN$, which displays two oxidation waves similar to those of $Co^{III}(TAAB^{2-})ClO_4$ but sharply different from that of $Co^{II}(TAAB)(ClO_4)_2$. A third oxidation process of $Co^{II}(TAAB^{2-})ClO_4$ at −0.92 V corresponds fairly well to the first reduction wave of $Co^{III}(TAAB^{2-})ClO_4$ at −1.06 V *vs.* Ag|0.1 *M* $AgNO_3$–CH_3CN. The fact that this oxidation and reduction form a couple is confirmed by CV studies on the first reduction wave of $Co(TAAB^{2-})ClO_4$ (Table II). The potential at 85% of the maximum peak height on the reduction half of the cycle,[28] $E_{1/2}r$, of the latter complex was determined to be −1.02 V. In the oxidation half of the cycle, $E_{1/2}a$ is calculated to be −0.95 V, which agrees favorably with the half-wave potential (−0.92 V) of the corresponding oxidation process for $Co^{II}(TAAB^{2-})\cdot CH_3CN$.

The above rearrangement reaction does not appear to be rapid, since in the electrochemical behavior of $Co^{II}(TAAB)^{2+}$ there is no evidence for the occurrence of the $Co^{I}(TAAB)^{+} \rightarrow Co^{III}(TAAB^{2-})^{+}$ transformation on a cyclic voltammetric time scale (times up to 2 min were investigated, using potential hold techniques). Such a reaction would be readily detected, since $Co^{III}(TAAB^{2-})^{+}$ exhibits unique redox behavior at +0.25 and −1.02 V, as previously noted. However by electrochemically monitoring a solution of $Co^{II}(TAAB)^{2+}$ which has been subjected to partial electrolysis (~15 min) at −0.95 V one finds direct evidence for the formation of $Co^{III}(TAAB^{2-})^{+}$ (Figure 6a). For comparison, the cyclic voltammogram of the oxidation and first reduction process of $Co^{II}(TAAB)^{2+}$ in acetonitrile solution is shown in Figure 6b. Apparently then, the time requirement for rearrangement was provided by electrolysis so that $Co^{III}(TAAB^{2-})^{+}$ was produced. In this context, it should be noted from the work of Oth,[7] that this is presumably the situation with regard to the aromatic dianion derived from [16]annulene, since under reducing conditions a fully developed nmr pattern attributed to the dianion structure is obtained only after ~36 hr at −30.0°. Unfortunately, the electrochemical behavior of this dianion was not reported.

Significant insight into the microscopic electrode behavior of $Co^{III}(TAAB^{2-})^{+}$ has been obtained through the further use of cyclic voltammetry. The number of processes which can be made to occur at the electrode surface can be controlled by simply limiting the span of the potential excursion which is applied to the electrochemical cell. When the two oxidation processes (E_p = +0.25 V and $E_{1/2}$ = +0.51 V) of $Co^{III}(TAAB^{2-})^{+}$ are excluded from its redox behavior in this manner, the only reduction wave seen is the expected one at $E_{1/2}$ = −1.02 V corresponding to

$$Co^{III}(TAAB^{2-})^{+} \underset{-e^-}{\overset{+e^-}{\rightleftharpoons}} Co^{II}(TAAB^{2-})^{0}$$

If, however, one or both of the oxidation processes of $[Co^{III}(TAAB^{2-})]^{+}$ is allowed to occur, then subsequent tracings of the current–potential curves reveal the appearance of two new reduction waves in the cathodic potential region of the polarogram (Figure 7). The potentials of these new waves (−0.85 and −1.22 V) correspond to the reduction potentials of the

$$Co^{II}(TAAB)^{2+} \underset{-e^-}{\overset{+e^-}{\rightleftharpoons}} Co^{I}(TAAB)^{+}$$

and

$$Co^{I}(TAAB)^{+} \underset{-e^-}{\overset{+e^-}{\rightleftharpoons}} Co^{0}(TAAB)^{0}$$

processes, respectively. This rather striking change in the current–potential curves of $Co^{III}(TAAB^{2-})^{+}$ unequivocally demonstrates the electrochemical link between the cobalt complexes of $TAAB^{2-}$ and those of TAAB and allows for more definite redox assignments in the cyclic voltammogram of $Co^{III}(TAAB^{2-})^{+}$.[29] These are included in the overall electrode sequences for the Co–TAAB complexes given in Figure 8, where A, B, and C are the compounds isolated and characterized and the numbers under the arrows identify each process with the appropriate $E_{1/2}$ as entered in Table II.

The postulated overall electrode reaction sequence of

(28) R. S. Nicholson and I. Shain, *Anal. Chem.*, 36, 706 (1964).

(29) In a previous report[1] we had erroneously stated that the second oxidation wave of $Co^{III}(TAAB^{2-})^{+}$ occurred at +0.70 V *vs.* $Ag|Ag^{+}$ (0.1 *M*). We now give +0.51 V as the correct observed value. In the same report we identified the two oxidation waves of $Co^{III}(TAAB^{2-})^{+}$ as ligand oxidations. However, in view of the present data, we prefer the reaction schemes given in the present text.

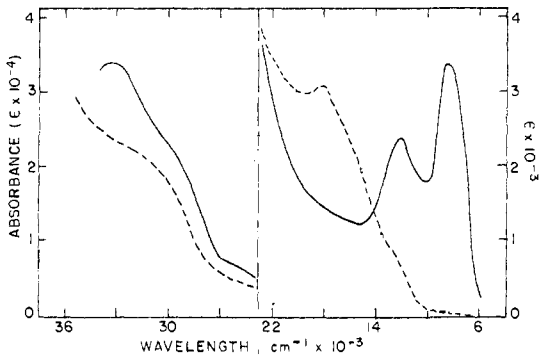

Figure 9. Electronic spectrum of $Co^{I}(TAAB)^{+}$ (solid line) and $Co(TAAB)ClO_4$ dissolved in acetonitrile solution (dotted line).

Figure 8 gains support from two considerations. First, the second oxidation process of $Co^{III}(TAAB^{2-})^{+}$ has an $E_{1/2}$ which appears to be identical with that of the first oxidation wave of the $Co^{II}(TAAB)^{2+}$ starting material, *i.e.*

$$Co^{II}(TAAB)^{2+} \underset{+e^-}{\overset{-e^-}{\rightleftharpoons}} Co^{III}(TAAB)^{3+}$$

This implies that the stable oxidation product at +0.25 V is $Co^{II}(TAAB)^{2+}$. A more graphic demonstration of this is seen from multiple scan cyclic voltammograms, as typified by Figure 7. Clearly from these curves, production of $Co^{II}(TAAB)^{2+}$ results from the first oxidation process of $Co^{III}(TAAB^{2-})^{+}$. The primary electrode product, written as $Co^{III}(TAAB\cdot^{-})^{2+}$, is apparently unstable with respect to $Co^{II}(TAAB)^{2+}$. This conversion must occur rapidly since the formation of $Co^{II}(TAAB)^{2+}$ is seen from cyclic voltammetric curves taken at potential scan rates up to 0.33 V/sec. This model is also consistent with the absence of a cathodic component for the oxidation wave at +0.25 V, since the first reduction wave of the ultimate oxidation product produced at +0.25 V, *i.e.*, $Co^{II}(TAAB)^{2+}$, does not occur until −0.85 V. This type of redox behavior has precedent, especially in the work of Adams and coworkers.[30,31] In their study of the electrochemical oxidation of aromatic amines and *p*-aminophenols, they found new waves appearing in multiple scan cyclic voltammograms, indicating the formation of electroactive hydrolysis and coupling products formed as a result of the initial electrode process.

The electronic spectrum of the initial electrode product, $Co(TAAB)^{+}$ ($Co^{I}(TAAB)^{+}$), can be obtained *in situ* by fairly rapid (5–10 min) electrolysis of a dilute solution (~1 mm) of $Co^{II}(TAAB)^{2+}$ on the plateau of its first reduction wave (−0.95 V). This generates a substantial amount of the unrearranged $Co^{I}(TAAB)^{+}$, and its electronic absorption spectrum is shown in Figure 9. It consists of a number of high intensity charge transfer transitions. For comparison, the spectrum of the isolated complex, $Co(TAAB)ClO_4$ is also given. Clearly the vast difference in these spectra suggest very different electronic structures for the ligand in the two different complexes. This is consistent with our formulation of $Co(TAAB)ClO_4$ as $[Co^{III}(TAAB^{2-})]ClO_4$. It is unfortunate that the spectrum

(30) D. Hawley and R. N. Adams, *J. Electroanal. Chem.*, **10**, 376 (1965).
(31) J. Bacon and R. N. Adams, *J. Amer. Chem. Soc.*, **90**, 6596 (1968).

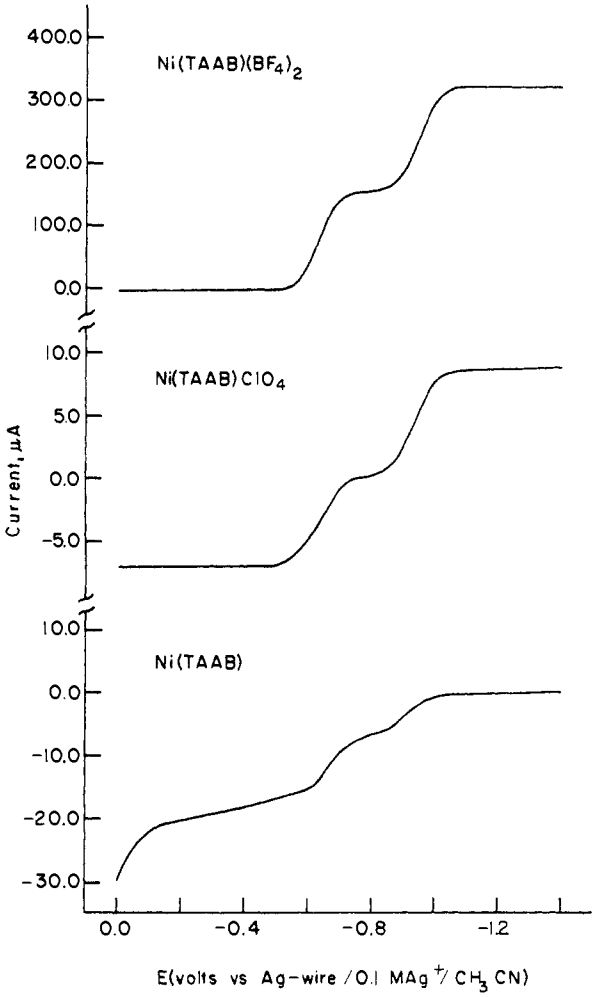

Figure 10. Rpe voltammograms of $Ni(TAAB)(BF_4)_2$, $Ni(TAAB)ClO_4$, and Ni(TAAB) in CH_3CN.

of this important complex is so broad and, consequently, of relatively little use in theoretical interpretation.

Voltammetric data on the oxidation and reduction products of $Ni^{II}(TAAB)^{2+}$ and $Cu^{II}(TAAB)^{2+}$ are given in Table II, and typical current–voltage curves of the products of $Ni^{II}(TAAB)^{2+}$ are shown in Figure 10. The half-wave potentials for these reversible redox processes agree with those of the parent complexes, as expected for Nernstian behavior for the couples. The electrochemically reversible nature of the $[M(TAAB)]^{+}$–$M(TAAB)^{0}$ couple, in both acetonitrile and methanol, suggests the improbability of an equilibrium of the type

$$[M(TAAB)]^{0} \rightleftharpoons M + \text{organic fragments}$$

Electron transfer reactions such as those described above are still quite unusual, although there is a growing number of literature reports concerning similar reactions. For example, an electron transfer reaction between metal and ligand has recently been reported[32] for the nickel tetraphenylporphyrin system, in which the $Ni^{III}(TPP^{2-})^{+}$ cation transforms in solution to the Ni(II) radical ion complex, $Ni^{II}(TPP\cdot^{-})^{+}$. Similarly, in redox studies of lead complexes of octaethylporphyrin, it was found that[33] the one-electron oxidation

(32) A. Wolberg and J. Monassen, *Inorg. Chem.*, **9**, 2365 (1970).
(33) J. A. Ferguson, T. J. Meyer, and D. G. Whitten, *Inorg. Chem.*, **11**, 2767 (1972).

product of $Pb^{II}(OEP^{-})^{+}$ yielded $Pb^{IV}(OEP^{2-})^{2+}$, clearly indicating an electron transfer from the lead ion to the oxidized porphyrin ligand. Still another example is illustrated by the reduction sequences of tetradehydrocorrin complexes of Co^{II}, which undergo electron transfer reactions[34] of the type[35]

$$Co^{I}(TDC^{-})^{0} \underset{-e^-}{\overset{+e^-}{\rightleftharpoons}} Co^{II}(TDC^{3-})^{-}$$

The electron transfer reactions displayed by the cobalt–TAAB system are to our knowledge unique, however, to the extent that the long lifetime of the redox intermediate (*i.e.*, $Co^{I}(TAAB)^{+}$) enables it to be clearly detected and characterized. This distinction is significant and the particular properties of the TAAB ligand which allow this may prove to be highly meaningful. On a broader scale, the increasing number of reported examples of intramolecular metal to ligand and ligand to metal electron transfer reactions may suggest a more general reactivity pattern than is presently realized, particularly with macrocyclic ligands.

Conclusions

We conclude that the complementary character of annulene-like and aromatic (porphyrin-like) ligands is well-illustrated by the foregoing studies. For both porphyrins and TAAB the general equation below holds

$$\text{aromatic dianion} \underset{+2e^-}{\overset{-2e^-}{\rightleftharpoons}} \text{tetraazaannulene}$$

The reasons for interest in this formulation are nontrivial. In such species as peroxidase and catalase, the functional forms of the heme prosthetic groups have undergone oxidation.[36] In some cases the oxidized forms may best be understood by thinking of their ligands as tetraazaannulenes, or derivatives thereof, rather than as aromatic ligands. Again the distinction is highly meaningful. The coordination site in a porphyrin (and related dianion ligand) is inflexible in the extreme. The metal ion site, size, and geometry are fixed to within a few per cent. Consequently, any changes involving a metal ion while in such sites must primarily depend on metal ion accommodation. For example, when an Fe(III) atom in a porphyrin ring is reduced to Fe(II) and subsequently reoxidized to Fe(III), it literally jumps in and out of the ring. This is because of the rigid geometry of the ring and because it apparently cannot alter its metal–nitrogen intervals by more than a few hundredths of an ångström. In contrast, the annulene-like ligand readily accommodates metal–donor internuclear distance changes of one- or two-tenths of an ångström, even with the same metal ion, while permitting the metal ion to remain essentially in a coplanar array with the four donor atoms.[15] While the full chemical significance of these distinctions remains to be clarified, they may be expected to be profound.

Experimental Section

Reagents. Methanol (Baler A. G.) was used for electrochemical studies without further purification. The acetonitrile employed similarly was purchased from Fisher Scientific Co., as well as from Matheson Coleman and Bell (Spectroquality, AS 145). It was purified by procedures described in the literature.[37,38] Purified acetonitrile was kept free from oxygen in a Dri-Train enclosure under a nitrogen atmosphere. Potassium chloride (Allied Chemical), potassium nitrate (Allied Chemical), and tetraethylammonium perchlorate(TEAP) and tetrabutylammonium iodide (TBAI) (both from Southwestern Analytical, Inc.) were used as supporting electrolytes. TEAP was purified by recrystallization from double distilled, demineralized water and dried over P_4O_{10} *in vacuo*, for several days before use. However, purification of TEAP by recrystallization did not improve the quality of the background polarogram.

The nitrogen gas used to deoxygenate the solutions was purchased from Burdett Oxygen Co. (99.96% pure). It was further purified by passing through a column packed with activated BASF catalyst, to remove the oxygen, then through a column packed with molecular sieves (5A) to remove the last traces of water. To suppress maxima for measurements in methanol, 0.1 ml of 0.02% solution of Triton X-100 (Rohm and Haas Co.) was employed.

All other chemicals used in this research were of analytical reagent grade and were used without further purification. The preparations of the cobalt, copper, and nickel complexes of TAAB were reported earlier.[8,19]

Physical Measurements. Infrared spectra were taken on a Perkin-Elmer Model 337 spectrophotometer using Nujol and Halo oil mulls.

Magnetic moments were determined under helium atmosphere by the Faraday method. Because the samples were sensitive to oxidation and moisture a glove box attachment for loading samples in an inert atmosphere was used. Conventional polarography was performed with a controlled potential and derivative voltammeter capable of electrolysis in a three-electrode configuration (Indiana Instrument and Chemical Corporation, Model ORNL-1988A). The recorder was a Hewlett-Packard/Moseley Division X-Y product (Model 2D2M). A dropping mercury electrode (dme) and a rotating platinum electrode (rpe) were used as the working electrodes. A platinum flag electrode served as the auxiliary electrode. The dme characteristics at a height of 50 cm were $t = 4.51$ sec and $m^{2/3} \cdot t^{1/6} = 1.92$ $mg^{2/3}\ t^{-1/6}$ at 0 V and $t = 4.41$ sec and $m^{2/3}t^{1/6} = 1.91$ $mg^{2/3}\ t^{-1/2}$ at -1.0 V *vs.* an aqueous saturated calomel electrode, sce. The rotating Pt electrode was driven by a 600 rpm synchronous motor (Welch Scientific Co.). A scan rate of 3.3 mV/sec was used with the dme and 6.6 mV/sec and 3.3 mV/sec with the rpe. The polarographic studies in methanol were carried out using millimolar concentrations of the electroactive species. For cyclic voltammetry, a platinum microsphere electrode (pmse) (0.13 cm in diameter), a stationary platinum wire (6 mm, 20 gauge), and a hanging mercury drop electrode (hmde) were used as the indicator electrodes.

For anhydrous studies an Ag wire, immersed in a 0.1 *M* $AgNO_3$–CH_3CN solution, constituted the reference electrode. The Ag wire| 0.1 *M* $AgNO_3$–CH_3CN reference electrode has been measured to have a potential of +0.36 V *vs.* sce.[39]

Electrochemical studies in methanol were made in conjunction with a saturated calomel electrode (sce) and a KCl-agar bridge. Unless otherwise stated, studies in methanol were carried out on solutions 0.05 *M* in background electrolyte.

In a typical experiment with methanol solvent, high purity nitrogen is passed first through an activated BASF catalyst to absorb the last traces of oxygen and then through a column packed with 5A molecular sieves to remove water. The nitrogen is bubbled through the polarographic solution for 25 min to remove dissolved oxygen, while simultaneously passing nitrogen over the surface of the solution. After this time, nitrogen is directed over only the surface of the solution for the duration of the polarographic determination. The measurements were made at 25 ± 0.2° utilizing a controlled temperature water bath, unless stated otherwise.

In some cases, coulometry at controlled potential was carried out in order to determine the exact number of electrons transferred. For the remaining complexes, an n value was determined by comparison of the respective diffusion currents with that for the coulometrically analyzed complexes. This is valid, since all of the complexes reported here are of similar size and geometry, and their diffusion coefficients should therefore be very similar.

(34) N. S. Hush, I. S. Woolsey, *J. Amer. Chem. Soc.*, **94**, 4107 (1972).
(35) Derivatives of tetradehydrocorrin.
(36) I. Yamazaki and K. Yokota, *Biochim. Biophys. Acta*, **105**, 301 (1965).
(37) E. O. Sherman and D. C. Olson, *Anal. Chem.*, 40, 1174 (1968).
(38) T. Osa and T. Kuwana, *J. Electroanal. Chem.*, **22**, 389 (1969).
(39) J. L. Mills, R. Nelson, S. G. Shore, and L. B. Anderson, *Anal. Chem.*, **43**, 157 (1971).

Controlled-Potential Electrolysis (cpe). For controlled-potential electrolysis a potentiostat (Brinkman-Wenking Electronic Potentiostat, Model 61-TR), as well as Model 68 FR 0.5, was employed.

The cell was designed and constructed for cpe in this department. The center compartment is shaped like a cylinder (60 mm diameter and 130 mm height). The working electrode, a Pt gauze electrode in this case, is placed in this compartment. Two side arms connect the working compartment to the other compartment by fine frits. One of the side arms contains the electrolyte solution, into which a salt bridge with a fine frit is immersed. Into this compartment the reference electrode, Ag wire|0.1 M $AgNO_3$–CH_3CN (for anhydrous electrolysis), is placed. This arrangement diminishes the diffusion of Ag^+ into the working compartment, particularly when one is careful with the heights of the liquid levels in different compartments. The other side arm has an inner and outer compartment. Both compartments contain background solution. The inner compartment which is 2 cm in length is separated from the outer compartment and working compartment by fine frits. The Pt auxiliary electrode is placed in the outer compartment. This arrangement minimizes the danger of mixing the products formed at the working and auxiliary electrodes. All electrolysis in acetonitrile is carried out in a Dri-Train (Vacuum Atmospheres Corporation) under nitrogen atmosphere since the reduction products are sensitive to oxygen and moisture while electrolysis in methanol was carried out on the bench using an sce as the reference electrode. Here, the solution was blanketed by nitrogen flow throughout the electrolysis.

Preparation of Ni(TAAB)ClO_4. Electroreduction of Ni(TAAB)-$(BF_4)_2$ to Ni(TAAB)ClO_4 was carried out in the Dri-Train enclosure in carefully purified acetonitrile. Approximately 200 ml of acetonitrile, which contained 0.05 M Et_4NClO_4 electrolyte, was placed in all the compartments of the electrolysis vessel, such that the liquid level in the ancillary compartments was about 0.5 in. higher than that in the working compartment to prevent flow under gravity of the background electrolyte and the compound into the side arms. A magnetic stirrer and a small stirring bar were employed to stir the solution vigorously. The solution was preelectrolyzed at a potential ~0.2 V more cathodic than the potential used in the subsequent electrolysis. The preelectrolysis was continued until the current dropped to ~0.02 μA. Then sufficient Ni(TAAB)$(BF_4)_2$ was added to the working compartment to make a 2×10^{-3} M solution and it was dissolved by stirring the solution with the magnetic stirrer. After Ni(TAAB)$(BF_4)_2$ was dissolved, the electrolysis was initiated by applying the desired potential (—0.75 V). The rpe, counter and reference electrodes were used in conjunction with the ORNL-1988A voltammeter and the recorder to obtain voltammograms at various time intervals during the cpe to check the extent and course of the electrolysis. During the course of electrolysis, the color of the solution turned from red to brown. After ~5 hr when the current dropped to approximately the value of the background solution (~0.02 μA), the electrolysis was stopped and the electrolyzed solution was transferred to a suction flask and the volume was reduced under reduced pressure until the electrolysis product began to separate from the solution. The brown crystals were filtered within the drybox, washed with acetonitrile, and vacuum dried on the filtering funnel. They were recrystallized from acetonitrile solution. *Anal.* Calcd for $C_{28}H_{20}N_4NiClO_4$: C, 58.83; H, 3.53; N, 9.82; Cl, 6.21; Ni, 10.29. Found: C, 59.15; H, 3.24; N, 9.96; Cl, 6.50; Ni, 10.08.

Preparation of Ni(TAAB). This compound was prepared in a similar way except that the reduction was carried out at −1.10 V *vs.* Ag wire|0.1 M Ag^+–CH_3CN. The electrolysis was completed after ~10 hr. Due to its low solubility in acetonitrile, Ni(TAAB) precipitates out during the electrolysis as a black-brown solid. After the electrolysis was completed, the subsequent work-up procedure is the same as for Ni(TAAB)ClO_4. *Anal.* Calcd for $C_{28}H_{20}Ni$: C, 71.37; H, 4.28; N, 11.89; Ni, 12.46. Found: C, 70.44, 70.35; H, 4.61, 4.13; N, 12.06, 11.93; Ni, 12.26.

Both Ni(TAAB)ClO_4 and Ni(TAAB), although sensitive to oxidation and moisture, can be stored in the solid state in a drybox for months.

During the attempt to synthesize the reduced nickel compounds it was found that highly purified acetonitrile is required for the electrolysis. Several experiments performed with insufficiently pure or dry acetonitrile have resulted in the formation of reduced species which are not stable over a long period of time or have produced undesirable products. The reduced species are not stable in methanol and attempts to produce them in that solvent led to the formation of Ni(TAAB)$(OMe)_2$. Presumably the reaction was

$$Ni(TAAB)^0 + 2CH_3OH \longrightarrow Ni^{II}(TAAB)(OCH_3)_2 + H_2$$

It is important to note at this point that attempted chemical reduction of the nickel ion in $Ni(TAAB)^{2+}$ has generally proven unsuccessful.[17] In fact, the product obtained by hydrogenation is $Ni(H_8TAAB)^{2+}$, not Ni(TAAB).[9]

Preparations of $Co^{III}(TAAB^{2-})ClO_4$ and $Co^{II}(TAAB^{2-})CH_3CN$. Anhydrous Co(TAAB)$(ClO_4)_2$ was used as the starting material for the electrolytic preparation of both reduced cobalt derivatives. The processes were carried out at constant potential using a Brinkman-Wenking Electronic Potentiostat Model 61-TR as well as a Model 68 FR 0.5 in a cell contained in a Vacuum Atmospheres Dri-Train enclosure, under a nitrogen atmosphere. In a typical preparation, 200 ml of 2×10^{-3} M solution of Co(TAAB)$(ClO_4)_2$ in CH_3CN was reduced at the desired potential (−0.95 V for Co(TAAB)ClO_4 and −1.35 V for Co(TAAB)·CH_3CN. Platinum gauze and flag were used as the working and auxiliary electrodes, respectively, and an $Ag|AgNO_3$ (0.1 M) electrode in CH_3CN was used as reference. The reduction process was monitored by determining voltammograms on the reacting solution, from time to time, using a stationary platinum electrode. During the course of the electrolysis the intense green color of $Co(TAAB)^{2+}$ changes to a deep brown-black color, the change being accompanied by the formation of a small quantity of an orange-brown precipitate. Both the one- and two-electron reduction products are black-looking crystalline solids. In the case of Co(TAAB)ClO_4 the solution was evaporated to about 40 ml before the product separated. The black solid was recrystallized from acetonitrile. After electrolysis Co(TAAB)·CH_3CN is extracted into dry hexane and the hexane is evaporated under reduced pressure in the Dri-Train enclosure until the product crystallizes. *Anal.* Calcd for Co-$(C_{28}H_{20}N_4)ClO_4$: C, 58.9; H, 3.53; N, 9.82; Cl, 6.21. Found: C, 59.6; H, 3.79; N, 9.96; Cl, 6.71. Calcd for $Co(C_{28}H_{20}N_4)$-CH_3CN: C, 70.3; H, 4.52; N, 13.7; Co, 11.5. Found: C, 69.7; H, 4.43; N, 14.4; Co, 11.6.

Synthesis of CoTAAB $(ClO_4)_2$. Boil $Zn(TAAB)ZnCl_4$ and $CoCl_2$ in ethanol for 3 hr. A green-brown precipitate of Co(TAAB)Cl_2 forms. This is converted to the NO_3^- salt by the addition of $NaNO_3$ and the product is caused to crystallize as CoTAAB $(ClO_4)_2$ by the addition of $NaClO_4$, yield 80%.

Acknowledgment. The financial support of the National Institutes of Health of the U. S. Public Health Service is greatly appreciated. Assistance was provided by Grant No. GM 10040.